NJC

Accepted Manuscript

This is an *Accepted Manuscript*, which has been through the Royal Society of Chemistry peer review process and has been accepted for publication.

Accepted Manuscripts are published online shortly after acceptance, before technical editing, formatting and proof reading. Using this free service, authors can make their results available to the community, in citable form, before we publish the edited article. We will replace this *Accepted Manuscript* with the edited and formatted *Advance Article* as soon as it is available.

You can find more information about *Accepted Manuscripts* in the Information for Authors.

Please note that technical editing may introduce minor changes to the text and/or graphics, which may alter content. The journal's standard Terms & Conditions and the Ethical guidelines still apply. In no event shall the Royal Society of Chemistry be held responsible for any errors or omissions in this *Accepted Manuscript* or any consequences arising from the use of any information it contains.

ROYAL SOCIETY OF CHEMISTRY

www.rsc.org/njc

Mesoporous silica SBA-15 functionalized with phosphonate derivatives for uranium uptake

Yu−Long Wang, Lu Zhu, Bo-Long Guo, Su-Wen Chen*, Wang-Suo Wu

School of Nuclear Science and Technology, Lanzhou University, Lanzhou, 730000, PR China

Abstract: Two functional SBA-15 were prepared by post-grafting method using phosphonate derivatives of diethylethylphosphonate (DEP) and ethylphosphonic acid (PA)，which were used as adsorbents for removal of uranium(VI) from aqueous solution. These materials were characterized by FT-IR, NMR, TEM, nitrogen adsorption/desorption experiments, and elemental analysis. The effect on uranium(VI) sorption behaviors of the functionalized SBA-15 was studied. Typical sorption isotherms (Langmuir and Freundlich) were determined for sorption process, and the maximum sorption capacity was calculated. The influence of organic functional groups on uranium(VI) sorption was also discussed. As a result, SBA-15-ethylphosphonic acid (SBA-15-PA) possessed not only a good sorption ability and a desirable selectivity for U(VI) over a range of competing metal ions but also a excellent reusability, which had potential application in separation of uranium(VI).

Keywords: Uranium; Sorption; SBA-15; Functionalization; Phosphonate derivatives

1. Introduction

In recent years, the mining and processing of uranium ores and the increasing use of nuclear power have created a legacy of contamination of uranium in soils and groundwater[1, 2]. Meanwhile, uranium is one of the most important heavy metals with chemical toxicity and radioactivity[3, 4], which causes progressive or irreversible renal injury and its compounds are potential carcinogens[5, 6]. Therefore, extraction and preconcentration of uranium(VI) from wastes are extremely important not only from the view of their limited resource availability but also for the reduction of their quantum for disposal as radioactive wastes[7]. For this purpose, numerous suitable treatment processes have been applied, including solvent extraction, precipitation, ion exchange, reverse osmosis, hyperfiltration, electrodialysis and sorption. Among them, sorption offers benefits of simplicity, rapidity, and easy recycling[8-11]. Consequently, the key is to discover the appropriate adsorbents for uranium.

In virtue of their large surface areas, high porosities, ordered pore arrangements, controllable, narrowly distributed pore size, and good hydrothermal stabilities, ordered mesoporous silica SBA-15 have drawn great interest in the research field of sorption since they were successfully synthesized by Zhao et al[12, 13]. However, the low chemical activity of SBA-15 surface cannot be ignored, which could result in the reduction of sorption ability. Thereby, many researchers modify SBA-15 with organic functional groups to improve its sorption ability and selectivity[14]. Acidichromic spiropyran-functionalized SBA-15 showed exceptional selectivity for adsorbing Am^{3+}

from aqueous solutions[15]. EDTA-PAMAM-functionalized SBA-15 showed a high affinity for many metal ions, such as Pb^{2+}, Zn^{2+}, Cu^{2+}, and Ni^{2+}[16]. G. E. Fryxell et al Lebed et al. reported that mesoporous silica supports functionalized with DiPhos, AcPhos, Prop-Phos, and 1,2-HOPO have a good sorption ability for lanthanides (La, Ce, Pr, Nd, Eu, Gd and Lu) from aqueous solution[17].

Hydroxyapatite have a good sorption ability for metal ions because of surface complexation on $\equiv$POH, precipitation of metal phosphates, ion exchange and sorption[18, 19]. Therefore, some reports have focused on technologies that can remove metal ions such as Pd(II), Cd(II), Zn(II), Co(II), Cu (II), Ba(II), and Sb(III) from contaminated soils, sediments, wastes and waste water by hydroxyapatite to protect the environment[20-22], radioactive elements Se (IV), Se(VI), Sr(II) and U(VI) have also been investigated[23-25]. Nevertheless, the application of hydroxyapatite on sorption areas was limited because the release of phosphate under some special conditions may be an important process for leading water eutrophication[26, 27], and its surface area is not large enough. Inspired by them, SBA-15-PA was synthesis by a post-grafting method in this work. It not only maintained the similar coordinating group on hydroxyapatite surface, improved chemical stability under some special conditions, but also increased the surface area. Hence, a good sorption ability of SBA-15-PA for uranium(VI) was expected. Coincidentally, the organo-functional group on SBA-15-diethylethylphosphonate (SBA-15-DEP) (the intermediate products during the synthesis of SBA-15-PA) surface is very similar to Tributyl phosphate (TBP), and TBP

as the solvent extraction reagent, has been used for a number of years to separate uranium and plutonium from irradiated fuel in PUREX process because of the good coordination ability[28]. Herein, the effect of various operational parameters such as pH, solid-liquid ratio, ionic strength, initial metal ion concentration, and temperature on uranium(VI) sorption behaviors of the functionalized SBA-15 was studied. Furthermore, the selective sorption ability of SBA-15, SBA-15-DEP, and SBA-15-PA were compared, and the influence of organic groups on SBA-15 surface on uranium(VI) sorption was also discussed.

2. Experimental

2.1. Reagents and materials

Mesoporous SBA-15 silica molecular sieves was obtained from unicarbonshanghai Co. Ltd. Toluene was distilled and dried before use according to conventional literature methods[29]. (2-diethylphosphatoethyl) triethoxysilane was purchased from Aladdin Inc. Other chemicals (ethanol, Me_3SiCl, HCl (12 mol/L)) used in the experiments are purchased as analytical purity or highest purity available, and used without any further purification. The water (resistance 18 MΩ cm^{-1}) used throughout the study has been deionized by means of a Millipore Milli-Q-system.

2.2. Synthesis of functionalized mesoporous silicates

The phosphonate derivatives functionalized SBA-15 were synthesized by post-grafting methods as per the procedure described below (Fig.1).

2.2.1. Synthesis of SBA-15-DEP

SBA-15-DEP was prepared as previously described[30].

14.0 g of the given activated SBA-15 (treated overnight at 100 °C under vacuum) was dispersed in 200 mL of dry toluene. Then, 21.0 mL of (2-diethylphosphatoethyl) triethoxysilane was added at once to the dispersion in toluene under nitrogen atmosphere at room temperature. The resulting mixture was left under further stirring for 24 h under reflux conditions. After cooling to room temperature, the suspended solid product was filtered, washed thoroughly with toluene and ethanol, then dried at 80 °C under vacuum overnight.

2.2.2. Synthesis of SBA-15-PA

SBA-15-PA was synthesized according to the procedure in the literature by acidolysis of SBA-15-DEP[31].

In order to avoid side reactions between the phosphonic acid groups and the surface Si-OH, silylation of Si-OH groups was first achieved by treating the SBA-15-DEP (17.35 g) with 50.0 mL Me_3SiCl in 200 mL dry toluene heated under reflux for 24 h. The solid (SBA-15-DEPP) was filtered, washed with dry toluene, then

dried at 80 °C under vacuum overnight.

18.45 g of SBA-15-DEPP was suspended in 200 ml of HCl (12 mol/L), the resulting mixture was left under further stirring for 24 h under reflux conditions. After cooling to room temperature, the solid product was washed thoroughly with water several times, then dried at 80 °C under vacuum overnight, SBA-15-PA was obtained.

2.3. Sorption experiments

The sorption of U(VI) from aqueous solutions onto SBA-15-DEP and SBA-15-PA at atmospheric pressure were studied by a batch method, including effects of the solution pH, solid-liquid ratio, ionic strength, initial metal ion concentration, and temperature. All sorption experiments were carried out in polyethylene centrifuge tubes. Stock solution of U(VI) was prepared by dissolving the appropriate amount of $UO_2(NO_3)_2{\cdot}6H_2O$ with concentrated nitric acid and then diluted to 2 mmol/L in 0.01 mol/L HNO_3 solution. In a typical experiment, appropriate volume of the suspension modified SBA-15, 0.16 mL $NaNO_3$ solutions (5 mol/L), 0.80 mL $UO_2(NO_3)_2{\cdot}6H_2O$ stock solutions, and a certain volume of H_2O were added (the total volume is 8.00 mL), after that pH values of the solution was adjusted to the desired values by using negligible volumes of NaOH and HNO_3 solutions, and stirring for 72 h at 298±1 K (Sorption equilibrium can be reached less than 10 hours for all materials through experiments). Then the suspension was centrifuged by centrifuge (H2050R-1, Xiang Yi centrifuge instrument Co. Ltd.) at 10280 g for 30 minutes. A certain volume of

supernatant was removed for U(VI) determined. The amount of U(VI) was estimated by spectrophotometry using Arsenazo(III) at 652 nm[32].

The sorption efficiency (E), and sorption capacity (q_e) of U(VI) were calculated as follows:

$$E(\%) = \frac{C_0 - C_e}{C_0} \times 100\% \qquad (1)$$

$$q_e = \frac{(C_0 - C_e)}{m_{sorbent}} \times V_{solution} \qquad (2)$$

Where C_0 (mol/L) and C_e (mol/L) represent the concentrations of U(VI) in the aqueous phase before and after the sorption equilibration, respectively; $m_{sorbent}$ (g) and $V_{solution}$ (L) represent the weight of adsorbent and the volume of the U(VI) solution used in the sorption experiment, respectively[33].

2.4. Characterization

FT-IR spectra were recorded on a Nexus-670 FT-IR spectrophotometer in the region 4000-400 cm^{-1} by using spectra quality KBr powder. The pure and functionalized SBA-15 were characterized by a FEI Tecnai F30 transmission electron microscope. Nitrogen adsorption/desorption isotherms of the adsorbents were obtained on a Micrometrics ASAP 2020 instrument at 77 K. The specific surface area was determined by applying the BET equation to the isotherm, and the pore size was obtained from the

maximum of the pore size distribution curve calculated by the Barrett–Joyner–Halenda (BJH) method using the adsorption branch of the isotherm. The total pore volume is evaluated by the single point method[34]. Organic group contents of the functionalized samples were determined using a Vario cude elemental analysis apparatus.

3. Results and discussion

3.1. Characterization of the adsorbents

Figure.2 shows the TEM images of the grafted and ungrafted SBA-15 materials. It shows that a well-ordered hexagonal array of mesopores can be seen when the electron beam is parallel to the main axis of the cylindrical pores and the parallel nanotubular pores can be seen when the electron beam is perpendicular to the main axis. It is illustrated in several reports that the hexagonal array of SBA-15 materials is highly ordered and stable[35]. Thus, these micrographs also support this idea. The TEM images confirmed the hexagonal crystal structure composed of one-dimensional channels. In addition, it was verified that the porous structure was not disrupted after the post-grafting synthesis.

Nitrogen gas adsorption-desorption isotherm tests were done to further investigate the changes of pore structure between SBA-15 and modified SBA-15. As shown in Figure.3 (a), all isotherms of SBA-15 samples are typical type IV exhibiting a sharp capillary condensation step and H1 hysteresis loop characteristic of large cylindrical

mesopores, which are obviously preserved after organic modification, implying the SBA-15 structure had been successfully remained. Figure.3 (b) is the BJH pore size distribution curves (acquired from the adsorption branch). The BET specific surface area, pore volume and pore size calculated using BJH model are listed in Table 1. The pore size of original SBA-15 support is the largest among three tested samples, while the SBA-15-DEP contains the smallest pore size. This can be seen from the P/P_0, at which capillary condensation steps took place. The BET specific surface area and pore volume are in the same order with pore size. The smallest of BET surface area, pore volume and pore size in SBA-15-DEP indicate that DEP derivatives were incorporated inside the pores of mesoporous framework and some of pores in SBA-15 are blocked during organic modification. The volume of PA derivatives are smaller than DEP derivatives, therefore, the BET surface area, pore volume and pore size in SBA-15-PA are smaller than SBA-15 and larger than SBA-15-DEP. It's important to note that although the peak position of BJH pore size distribution curve for SBA-15-PA is smaller than SBA-15, the pore size distribution get wider. This is due to the partial structural collapse of silica framework during the acidolysis of SBA-15-DEP. These results confirmed that of SBA-15 was successful modified, based on the published work[36].

Fig.4 shows the FT-IR patterns of adsorbents. SBA-15 shows the typical adsorption bands of the SBA-15 silica at 1080 cm^{-1} (asymmetric Si-O-Si stretch), 804 cm^{-1} (symmetric Si-O-Si stretch), and 461cm^{-1} (Si-O-Si bending mode), while the

adsorption bands at 3437 cm^{-1} and 1635 cm^{-1} are assigned to hydrated silane group and the bending vibration of surface hydroxide[37], respectively. On the other hand, functionalized SBA-15 presented characteristic bands for aliphatic C-H stretching vibrations for pendant alkyl chains around 3000-2800 cm^{-1}[29]. These results indicate that SBA-15 was modified with phosphonate derivatives.

Fig.5 shows the ^{13}C CP-MAS NMR spectra of SBA-15 materials grafting with phosphonate derivatives. All the resonance signals in the ^{13}C CP-MAS NMR spectra can be assigned to appropriate C atoms, as denoted. The results clearly confirm that two kinds of iminodiacetic acid derivatives grafted SBA-15 materials, namely SBA-15-DEP and SBA-15-PA have been successfully prepared[30].

The content of C and H in SBA-15-DEP has been determined by element analysis. The amount of organic functional groups grafted on SBA-15-DEP surface was determined by the elemental analysis. For SBA-15-DEP, it was in accordance with the result of C elemental analysis and the final modified group was diethylethylphosphonate. The concentration of organic functional groups based on C elemental analysis for SBA-15-DEP was 0.989 mmol/g.

3.2. Sorption behavior studies

3.2.1. The effect of pH value on sorption behavior

The pH value of solution is an important parameter that influences the metal ion sorption, because it affects the speciation of metal ions (Fig.6 (a)) as well as the surface charge and binding sites of the adsorbent remarkably[38]. Here, sorption experiments were carried out at the pH of 1.5-7.0, while keeping other parameters constant. As shown in Fig.6 (b), the U(VI) sorption ability of unmodified and modified SBA-15 were dependent on the pH value significantly.

There was no obvious sorption of uranyl ions (UO_2^{2+}) on SBA-15 when the pH value was less than 3.0, the sorption percentage increased sharply with the increase of pH from 3.0 to 5.5, and quantitative sorption was obtained when the pH value was above 5.5. At low pH value, species of U(VI) in solution and the form of surface hydroxyl groups (Si-OH) were influenced by pH greatly[34]. When pH is greater than 5.0, precipitation of the metal hydroxide is expected. To avoid severe hydrolysis and precipitation of U(VI) from the solution at higher pH, pH = 4.00±0.02 was selected for further sorption experiments.

At low pH, U(VI) is known to exist as UO_2^{2+} in the solution, whereas the phosphonate groups, acting as binding sites on SBA-15-DEP are protonated and positively charged. Owing to the electrostatic repulsion, the positively charged UO_2^{2+} is not favored by the positively charged binding groups, resulting in a lower sorption ability. As the pH increases, the phosphonate group is deprotonated, whereas U(VI) still exists in a positively charged form. The electrostatic interaction and complexation between the O in the phosphonate moiety and U(VI) leads to the increase of the sorption

ability. On the other hand, the species distribution of U(VI) is greatly dependent on the solution pH[39].

For SBA-15-PA, the ascending branch of the Sorption-pH curves were wider, and the sorption percentage were higher than SBA-15 and SBA-15-DEP. This may be attributed to the presence of phosphonate ($PO(OH)_2^-$) suitable for coordination with the metal ion. The decrease of uptake in acidic media may be attributed to the lower dissociation extent of the phosphonate group, which hinder the interaction of metal ion[40].

3.2.2. The effect of solid-to-liquid ratio on sorption behavior

The distribution of U(VI) adsorbed on three kinds of materials as a function of solid-to-liquid ratio is shown in Fig.7 (a). The amount of U(VI) removal from solution increases obviously with the addition of adsorbents at low solid-to-liquid ratio, while increases slightly at high solid-to-liquid ratio for all materials. The improved sorption is due to the increased sites for binding to U(VI), which enhances the sorption of U(VI) from solution to solid[41]. In addition, for SBA-15-DEP, it exhibits a lower sorption ability than pure SBA-15, which could be due to the spatial configuration of functional groups on SBA-15-DEP surface and channel plugging in the course of grafting, but SBA-15-PA exhibits a exciting sorption ability, only 0.15 g/L SBA-15-PA was needed when the sorption percentage was about 50%, and for SBA-15 the solid-to-liquid ratio was 2 g/L in the same condition.

3.2.3. The effect of ionic strength on sorption behavior

The influence of $NaNO_3$ concentration on the U(VI) sorption ability of three kinds of materials are shown in Fig.7 (b). The U(VI) sorption ability decreased with the $NaNO_3$ concentration increasing from 0.01 to 0.10 mol/L, and remained constant when the concentration of $NaNO_3$ was higher for SBA-15. From these results, it can be concluded that the U(VI) sorption ability of the unmodified SBA-15 materials is greatly influenced by ionic strength when concentration of $NaNO_3$ is low. This is because the double layer thickness on adsorbents surface and the interface potential decreased with the increasing concentration of $NaNO_3$, thereby the sorption property of adsorbents for U(VI) decreased. The competition between increasing Na^+ ions and U(VI) ions for the active sites on sorbents might also be responsible for the decrease of U(VI) sorption[42]. For SBA-15-DEP and SBA-15-PA, the concentration of $NaNO_3$ has no influence on the sorption percentage of U(VI). Compared with inner-sphere surface complexes, outer-sphere complexes are more easily affected by the variations of ionic strength[43]. Consequently, the sorption of U(VI) is assumed to form the outer-sphere surface complexes for SBA-15 and inner-sphere surface complexes for SBA-DEP and SBA-15-PA, respectively.

3.2.4. Sorption isotherms

Temperature is an important parameter that affects the physicochemical behavior of metal ions in the environment. The sorption equilibrium isotherm is an important

parameter that demonstrates how the adsorbate molecules distribute between the liquid and the solid phases when the sorption process reaches an equilibrium state[44].

The equilibrium experiments were performed on SBA-15, SBA-15-DEP, and SBA-15-PA with the U(VI) concentration varying from 2.00×10^{-5} to 1.20×10^{-3} mol/L, and the pH value was selected at 4.00±0.02 in order to avoid the occurrence of insoluble U(VI) species (see Fig.8). The sorption data were modeled using the two frequently used isotherm models, namely Langmuir and Freundlich isotherms (Fig.9 (a) and (b)), to describe the experimental results and the real sorption behavior.

The Langmuir isotherm and the Freundlich isotherm can be represented by following equations[45].

$$\frac{C_e}{q_e} = \frac{C_e}{q_{max}} + \frac{1}{K_L} \qquad (3)$$

$$\lg q_e = \lg K_F + n\lg C_e \qquad (4)$$

Where q_{max} (mol/g) and q_e (mol/g) are the maximum sorption capacity and the equilibrium sorption capacity, respectively. C_e (mol/L) is the equilibrium concentration in supernatant, K_L (L/g) is sorption equilibrium constant, K_F ($mol^{1-n}\ L^n\ g^{-1}$) represents the sorption capacity when adsorbate equilibrium concentration equals to 1, and n is the degree of sorption dependence at equilibrium concentration.

Fig.8 shows that the sorption ability for all kinds of materials increased with the concentration of U(VI) increasing. In addition, the U(VI) sorption ability of SBA-15 decreased with the temperature increasing, demonstrating that the sorption process is an exothermic process. However, for functionalized SBA-15 materials, sorption ability increased with the temperature increasing, indicating that the sorption was an endothermic process. The isotherms of Langmuir and Freundlich models for the U(VI) sorption on all materials operated at 298±1 K are shown in Fig.9, and the corresponding parameters are listed in Table 2. It can be seen that SBA-15-PA exhibited a enhanced maximum sorption capacity than that of pure SBA-15. However, as for SBA-15-DEP, the maximum sorption capacity is lower than pure SBA-15 due to the large steric hindrance group of the DEP and channel plugging in the course of grafting.

3.2.5. Selectivity test

We also investigated the selectivity of the unmodified and modified SBA-15 materials by sorption of U(VI) from the aqueous solution containing other competing metal ions. The selectivity test was performed at aqueous solution containing U(VI), Ba^{2+}, Cs^{+}, Sr^{2+}, Ag^{+}, Cd^{2+}, and Co^{2+} at pH value about 4.00±0.02. The concentration of residual tested ions in supernatants after test was determined by ICP-AES. As shown in Fig.10, SBA-15-PA exhibited a improved selective sorption ability and lower sorption ability for other competing metal ions to SBA-15 and SBA-15-DEP. Taking into account the solubility product constants of the metal ions-phosphate compound, it is reasonable that the PA derivatives functionalized SBA-15 have strong selective

adsorption ability to U(VI). The result is well consistent to the solubility product constants of the metal ions-phosphate compound in some literature[46] (For example, Cs_3PO_4 is soluble in water; the solubility product constants are pK_{sp} = 46.7, 22.47, 27.39, 16.05, 32.6 and 34.69 for $(UO_2)_3(PO_4)_2$, $Ba_3(PO_4)_2$, $Sr_3(PO_4)_2$, Ag_3PO_4, $Cd_3(PO_4)_2$ and $Co_3(PO_4)_2$, respectively). It is worth reminding that, the selective sorption ability of SBA-15-PA may have potential application prospect in U(VI) separation area.

3.2.6 Release Behavior and Reusability of SBA-15-PA

Considering, SBA-15-PA showed not only a good sorption ability but also a desirable selectivity for U(VI) over a range of competing metal ions above, the study on release behavior and reusability of SBA-15-PA is essential. It concerns the use of this adsorbent in practice and use conditions. Release behavior test of SBA-15-PA was divided into two steps: (1) SBA-15-PA was reached sorption equilibrium with U(VI) solutions under following conditions: $C_{0U(VI)}$ = 4.00E-4 mol/L, $m/V_{(SBA\text{-}15\text{-}PA)}$ = 2.0 g/L, C_{NaNO3} = 0.1 mol/L, T = 298±1 K. (2) The U(VI) release percentage from SBA-15-PA was studied as a function of pH (pH values of the solution was adjusted by using NaOH and HNO_3 solutions). It is clear, when the pH value was less than 3.0, release percents of U(VI) decreased with the pH increasing; there was no obvious release of UO_2^{2+} on SBA-15-PA when the pH value was above 3.0 (Fig.11 (a)). This is because the dissociation of U-phosphate compound and recovery of phosphonate ($PO(OH)_2-$) on SBA-15-PA surface are easier under low pH values.

In order to check the reusability of the adsorbent, SBA-15-PA was subjected to several loading ($C_{0U(VI)}$ = 4.00E-4 mol/L, $m/V_{(SBA-15-PA)}$ = 2.0 g/L, C_{NaNO3} = 0.1 mol/L, T = 298±1 K) and elution experiments (HNO_3 solutions, pH = 0). The capacity of the SBA-15-PA was found to be practically constant (above 99%) after 6 times repeated use (Fig.11 (b)); thus multiple use of the adsorbent was seen to be feasible.

4. Conclusion

Two phosphonate derivatives functionalized SBA-15 materials have been synthesized by a post-grafting method, and their sorption behaviors of U(VI) from aqueous solution were investigated by batch techniques. The sorption of U(VI) on pure and modified SBA-15 were studied as a function of various parameters such as pH, solid-to-liquid ratio, ionic strength, U(VI) concentration, and temperature. U(VI) sorption ability of all adsorbents is strongly dependent on pH values. Outer-sphere complexation for SBA-15 and inner-sphere complexation for SBA-15-DEP and SBA-15-PA may be the main sorption mechanism of U(VI), respectively. The sorption isotherm has been successfully modeled by the Langmuir isotherm, which reveals a monolayer chemical sorption of U(VI) on modified SBA-15, but Freundlich isotherm is better for SBA-15, it indicates that different sites with several sorption energies are involved. SBA-15-PA showed not only a good sorption ability and a desirable selectivity for U(VI) over a range of competing metal ions but also a excellent reusability, it may have potential application prospect in U(VI) separation area.

Acknowledgments

This work was supported by National Natural Science Foundation of China (21101082, J1210001) and Fundamental Research Funds for the Central University (Lzujbky-2013-55).

Reference

[1] K. Maher, J. R. Bargar and G. E. *Brown, Inorg. Chem.*, 2013, 52, 3510-3532.

[2] P. J. Lebed, J. D. Savoie, J. Florek, F. Bilodeau, D. Lariviere and F. Kleitz, *Chem. Mater.*, 2012, 24, 4166-4176.

[3] M. Wazne, G. P. Korfiatis and X. G. Meng, *Environ. Sci. Technol.*, 2003, 37, 3619-3624.

[4] E. S. Ilton, Z. Wang, J. F. Boily, O. Qafoku, K. M. Rosso and S. C. Smith, *Environ. Sci. Technol.*, 2012, 46, 6604-6611.

[5] B. E. Johnson, P. H. Santschi, C. Y. Chuang, S. Otosaka, R. S. Addleman, M. Douglas, R. D. Rutledge, W. Chouyyok, J. D. Dacidson, G. E. Fryxell and J. M. Schwantes, *Environ. Sci. Technol.*, 2012, 46, 11251-11258.

[6] H. B. Jung, M. I. Boyanov, H. Konishi, Y. Sun, B. Mishra, K. M. Kemner, E. E.

Roden and H. Xu, *Environ. Sci. Technol.*, 2012, 46, 7301-7309.

[7] H. J. Park and L. L. Tavlarides, *Ind. Eng. Chem. Res.*, 2010, 49, 12567-12575.

[8] A. M. Donia, A. A. Atia, T. E. Amer, M. N. E. Hazek and M. H. Ismael, *J. Dispersion Sci. Technol.*, 2011, 32, 1673-1681.

[9] S. D. Yusan and S. Akyil, *J. Hazard. Mater.*, 2008, 160, 388-395.

[10] S. R. Sabale, D. V. Jadhav and B. S. Mohite, *J. Radioanal. Nucl. Chem.*, 2010, 284, 273-278.

[11] J. R. Memon, K. R. Hallam, M. I. Bhanger, A. E. Turki and G. C. Allen, *Ana. Chim. Acta*, 2009, 631, 69-73.

[12] D. Y. Zhao, J. L. Feng, Q. S. Huo, N. Melosh, G. H. Fredrickson, B. F. Chmelka and G. D. Stucky, *Science*, 1998, 279, 548-552.

[13] D. Y. Zhao, Q. S. Huo, J. L. Feng, B. F. Chmelka, and G. D. Stucky, *J. Am. Chem. Soc.*, 1998, 120, 6024-6036.

[14] M. Li, P. J. Pham, C. U. Pittman and T. Li, *Microporous Mesoporous Mater.*, 2009, 117, 436-443.

[15] C. T. Burns, S. Y. Choi, M. L. Dietz and M. A. Firestone, *Sep. Sci. Technol.*, 2008, 43, 2503-2519.

[16] Y. Jiang, Q. Gao, H. Yu, Y. Chen and F. Deng, *Microporous Mesoporous Mater.*, 2007, 103, 316-324.

[17] W. Yantasee, G. E. Fryxell, R. S. Addleman, R. J. Wiacek, V. Koonsiripaiboon, K. Pattamakomsan, V. Sukwarotwat, J. Xu, K. N. Raymond, *Journal of Hazardous Materials*, 2009, 168, 1233-1238.

[18] R. H. Zhu, R. B. Yu, J. X. Yao, D. Mao, C. J. Xing and D. Wang, *Catal. Today*, 2008, 139, 94-99.

[19] A. Corami, S. Mignardi and V. Ferrini, *J. Colloid Interface Sci.*, 2008, 317, 402-408.

[20] P. K. Chaturvedi, C. S. Seth and V. Misra, *Chemosphere*, 2006, 64, 1109-1114.

[21] Y. Hashimoto, T. Taki and T. Sato, *J. Environ. Manage.*, 2009, 90, 1782-1789.

[22] A. G. Leyva, J. Marrero, P. Smichowski and D. Cicerone, *Environ. Sci. Technol.*, 2001, 35, 3669-3675.

[23] S. Raicevic, Z. Vukovic, T. L. Lizunova and V. F. Komarov, *J. Radioanal. Nucl.*

Chem., 1996, 204, 363-370.

[24] M. Duc, G. Lefevre, M. Fedoroff, J. Jeanjean, J. C. Rouchaud, F. M. Rivera, J. Dumonceau and S. Milonjic, *J. Environ. Radioactiv.*, 2003, 70, 61-72.

[25] J. S. Arey, J. C. Seaman and P. M. Bertsch, *Environ. Sci. Technol.*, 1999, 33, 337-342.

[26] N. T. Basta and S. L. M. Gowen, *Environ. Pollut.*, 2004, 127, 73-82.

[27] S. B. Chen, Y. G. Zhu and Y. B. Ma, *J. Hazard. Mater.*, 2006, 134, 74-79.

[28] P. B. Iveson, M. G. B. Drew, M. J. Hudson and C. Madic, *J. Chem. Soc., Dalton Trans.*, 1999, 3605-3610.

[29] D. P. Quintanilla, I. D. Hierro, M. Fajardo and I. Sierra, *J. Hazard. Mater.*, 2006, 134, 245-256.

[30] Y. C. Pan, H. H. G. Tsai, J. C. Jiang, C. C. Kao, T. L. Sung, P. J. Chiu, D. Saikia, J. H. Chang and H. M. Kao, *J. Phys. Chem. C*, 2012, 116, 1658-1669.

[31] R. J. P. Corriu, L. Datas, Y. Guari, A. Mehdi, C. Reye and C. Thieuleux, *Chem. Commun.*, 2001, 763-734.

[32] C. S. K. Raju and M. S. Subramanian, *J. Hazard. Mater.*, 2007, 145, 315-322.

[33] Y. L. Liu, L. Y. Yuan, Y. L. Yuan, J. H. Lan, Z. J. Li, Y. X. Feng, Y. L. Zhao, Z. F. Chai and W. Q. Shi, *J. Radioanal. Nucl. Chem.*, 2011, 292, 803-810.

[34] H. Sepehrian, M. Samadfam and Z. Asadi, *Environ. Sci. Technol.*, 2012, 9, 629-636.

[35] F. Sevimli and A. Yılmaz, *Microporous Mesoporous Mater.*, 2012, 158, 281-291.

[36] H. Zhao, W. Li, M. Du, X. Pu and X. Shao, *Mater. Lett.*, 2013, 92, 33-35.

[37] J. Aguado, J. M. Arsuaga, A. Arencibia, M. Lindo and V. Gascon, *J. Hazard. Mater.*, 2009, 163, 213-221.

[38] I. M. E. Nahhal, F. R. Zaggout and M. A. Nassar, *J. Sol-Gel Sci. Technol.*, 2003, 28, 255-265.

[39] X. L. Wang, L. Y. Yuan, Y. F. Wang, Z. J. Li, J. H. Lan, Y. L. Liu, Y. X. Feng, Y. L. Zhao, Z. F. Chai and W. Q. Shi, *Sci. China Chem.*, 2012, 55, 1705-1711.

[40] C.Y. Chen, C. L. Chiang and P. C. Huang, *Sep. Purif. Technol.*, 2006, 50, 15-21.

[41] G. D. Sheng, J. Hu and X. K. Wang, *Appl. Radiat. Isot.*, 2008, 66, 1313-1320.

[42] C. L. Chen and X. K. Wang, *Appl. Geochem.*, 2007, 22, 436-445.

[43] D. M. Singer, K. Maher and G. E. Brown, *Geochim. Cosmochim. Acta*, 2009, 73, 5989-6007.

[44] S. W. Chen, B. L. Guo, Y. L. Wang, Y. Li and L. J. Song, *J. Radioanal. Nucl. Chem.*, 2012, 295, 1435-1442.

[45] Y. Y. Zhang, H. G. Zhao, Q. H. Fan, X. B. Zheng, P. Li, S. P. Liu and W. S. Wu, *J. Radioanal. Nucl. Chem.*, 2011, 288, 395-404.

[46] J. G. Speight, *Lange's Handbook of Chemistry*, McGraw-Hill Companies, Laramie, Wyoming, Sixteenth Edition , 2004, pp. 331-342.

Figure captions

Fig.1. Schematic illustration of the synthesis process of SBA-15-DEP and SBA-15-PA.

Fig.2. TEM images of (a) (b) SBA-15, (c) SBA-15-DEP, and (d) SBA-15-PA.

Fig.3. (a) N_2 adsorption-desorption isotherms of pure and modified SBA-15 samples. (b) BJH pore size distribution curves (acquired from the adsorption branch).

Fig.4. FT-IR spectra of adsorbents.

Fig.5. Solid state ^{13}C CP-MAS NMR spectra of (a) SBA-15-DEP and (b) SBA-15-PA.

Fig.6. (a) The relative species distribution of UO_2^{2+} in presence of CO_2 (by calculation). $C_{0U(VI)}$ = 2.00E-4 mol/L. (b) The effect of solution pH value on U(VI) sorption ability to adsorbents. $C_{0U(VI)}$ = 2.00E-4 mol/L, $m/V_{(SBA-15)}$ = 1.5 g/L, $m/V_{(SBA-15-DEP)}$ = 2.5 g/L, $m/V_{(SBA-15-PA)}$ = 0.15 g/L, C_{NaNO3} = 0.1 mol/L, T = 298±1 K, t = 72 h.

Fig.7. (a) The effect of solid-to-liquid ratio on sorption behavior. $C_{0U(VI)}$ = 2.00E-4 mol/L, C_{NaNO3} = 0.1 mol/L, T = 298±1 K, pH = 4.00±0.02, t = 72 h. (b) The effect of ionic strength on U(VI) sorption ability to adsorbents. $C_{0U(VI)}$ = 2.00E-4 mol/L, $m/V_{(SBA-15)}$ = 0.5 g/L, $m/V_{(SBA-15-DEP)}$ = 2.5 g/L, $m/V_{(SBA-15-PA)}$ = 0.15 g/L, T = 298±1 K, pH = 4.00±0.02, t = 72 h.

Fig.8. Sorption isotherms of U(VI) onto (a) SBA-15, (b) SBA-15-DEP, and (c) SBA-15-PA, C_{NaNO3} = 0.1 mol/L, $m/V_{(SBA-15)}$ = 0.5 g/L, $m/V_{(SBA-15-DEP)}$ = 2.5 g/L, $m/V_{(SBA-15-PA)}$ = 0.15 g/L, pH = 4.00±0.02, t = 72 h.

Fig.9. The isotherms of (a) Langmuir and (b) Freundlich models for U(VI) sorption. C_{NaNO3} = 0.1 mol/L, $m/V_{(SBA-15)}$ = 0.5 g/L, $m/V_{(SBA-15-DEP)}$ = 2.5 g/L, $m/V_{(SBA-15-PA)}$ = 0.15 g/L, T = 298±1 K, pH = 4.00±0.02, t = 72 h.

Fig.10. Competitive sorption of coexistent ions. $C_{0U(VI)}$ = 1.61E-4 mol/L, $C_{0Ba(II)}$ = 1.76E-4 mol/L, $C_{0Cs(I)}$ = 1.98E-4 mol/L, $C_{0Sr(II)}$ = 1.70E-4 mol/L, $C_{0Ag(I)}$=1.50E-4 mol/L, $C_{0Cd(II)}$=2.00E-4 mol/L, $C_{0Co(II)}$=2.73E-4 mol/L, C_{NaNO3} = 0.1 mol/L, pH= 4.00±0.02, T = 298±1 K, t = 72 h.

Fig.11. (a) Release efficiencies of U(VI) vs pH on SBA-15-PA in solutions. (b) Reusability tests of SBA-15-PA.

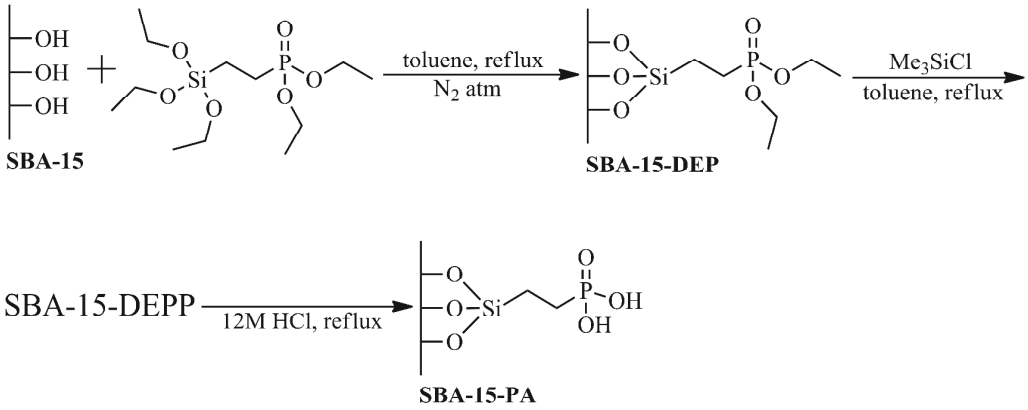

Fig.1.

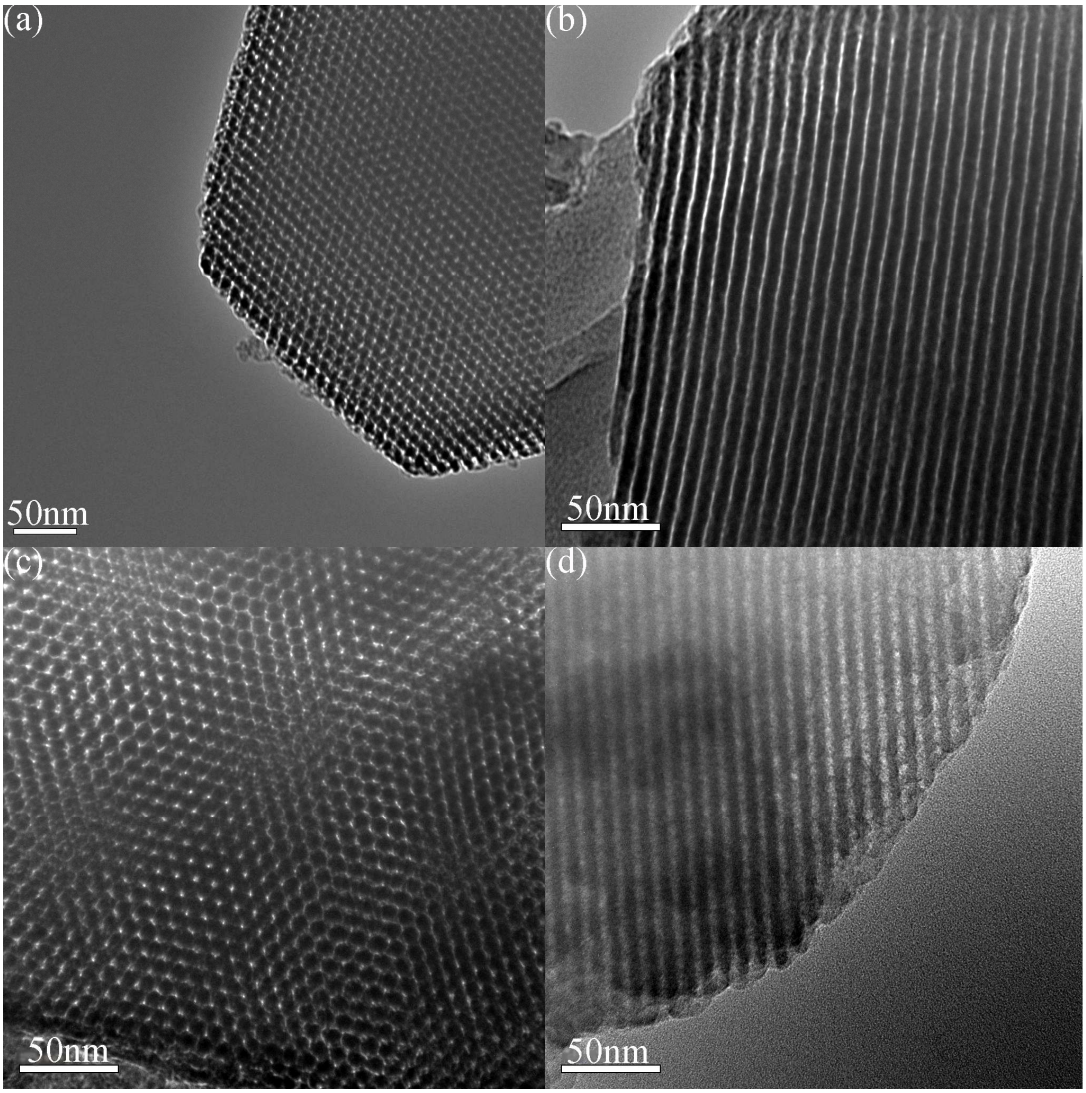

Fig.2.

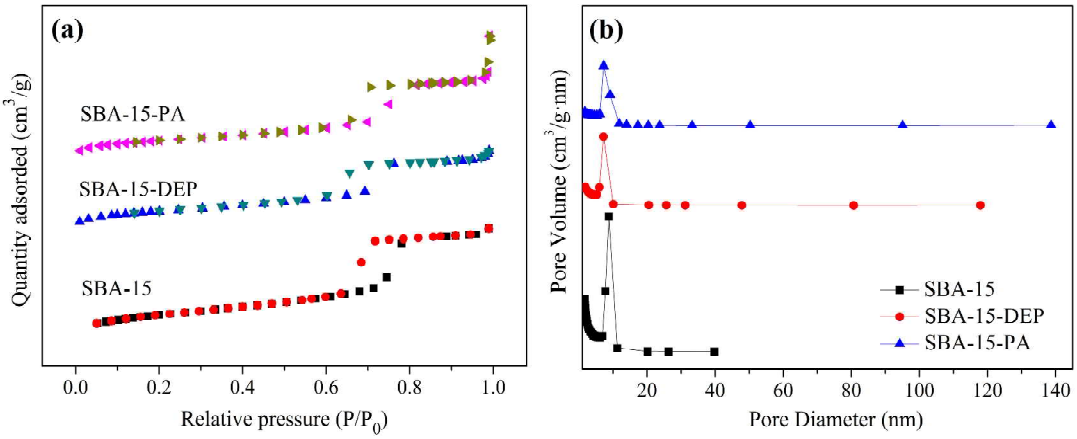

Fig.3.

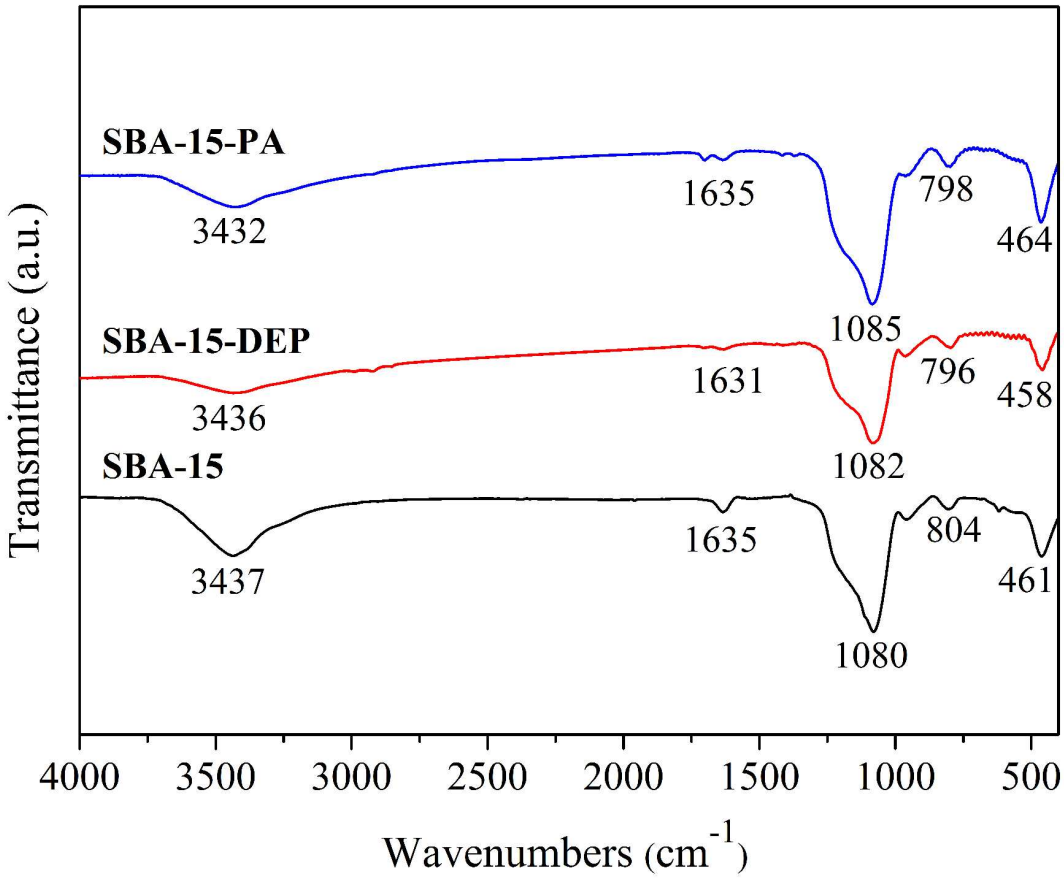

Fig.4.

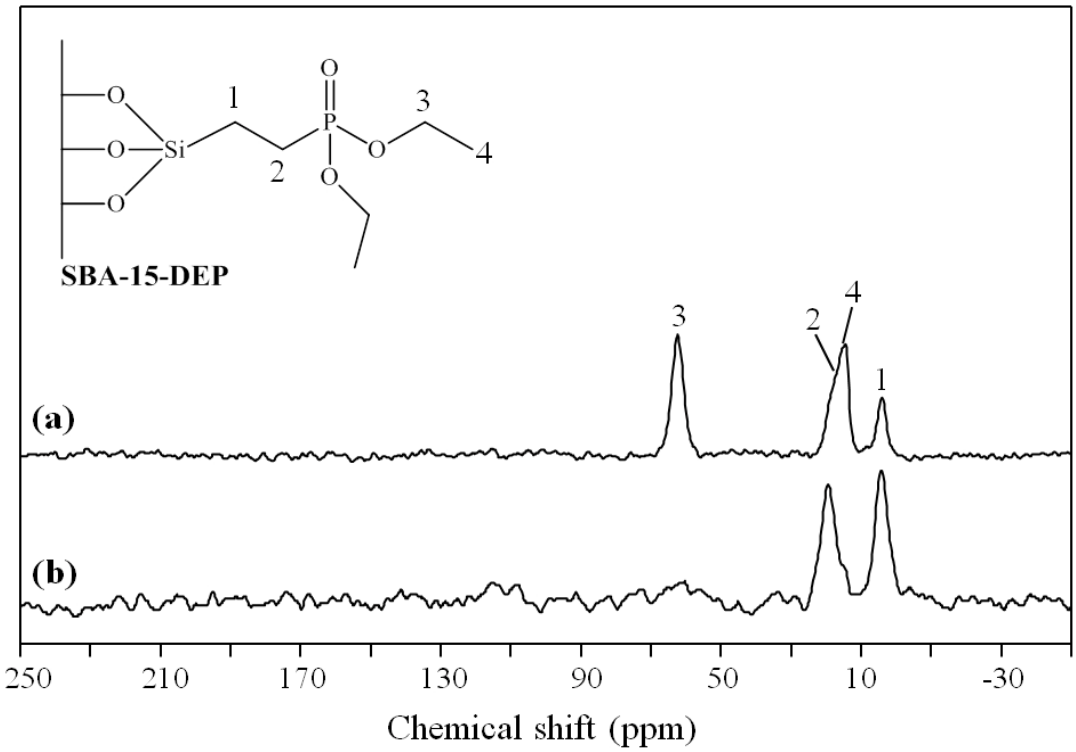

Fig.5.

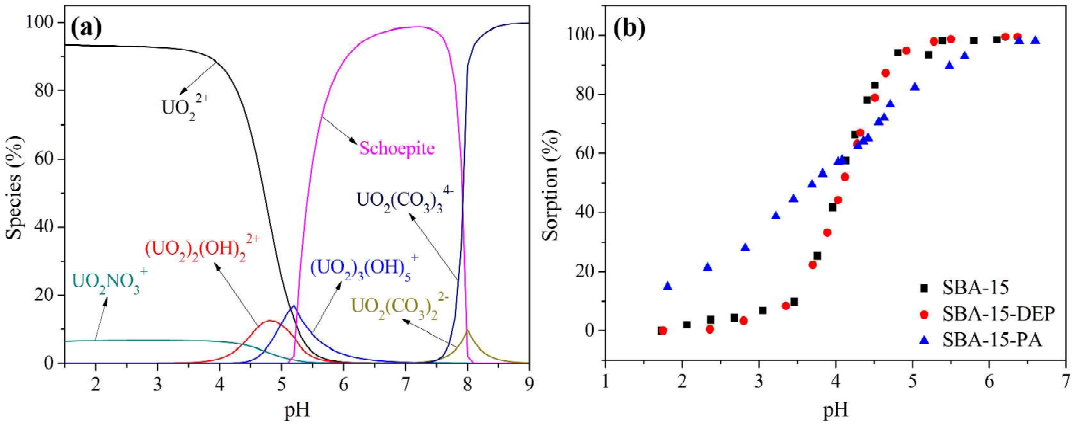

Fig.6.

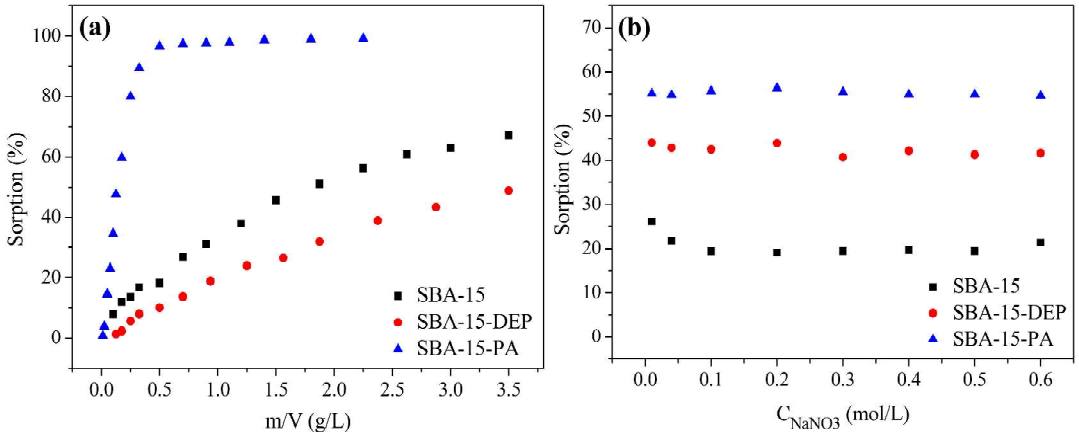

Fig.7.

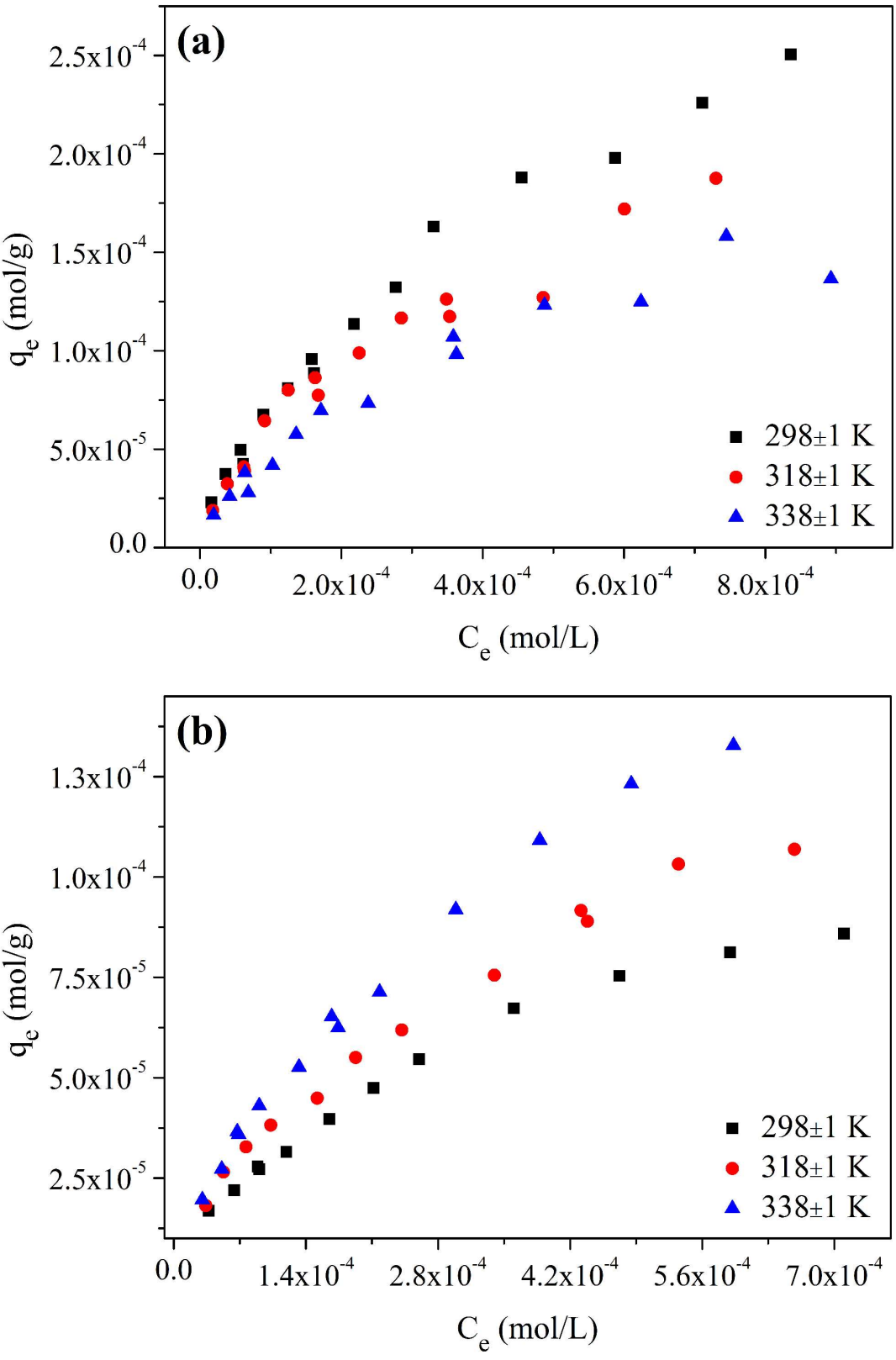

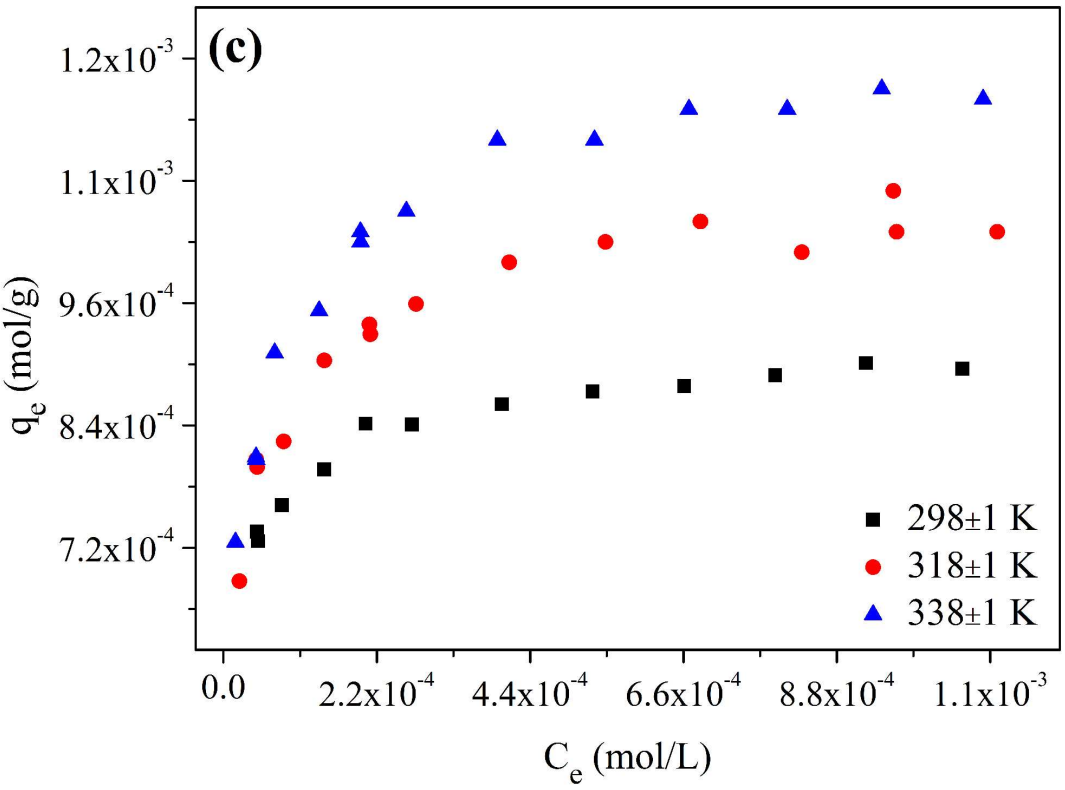

Fig.8.

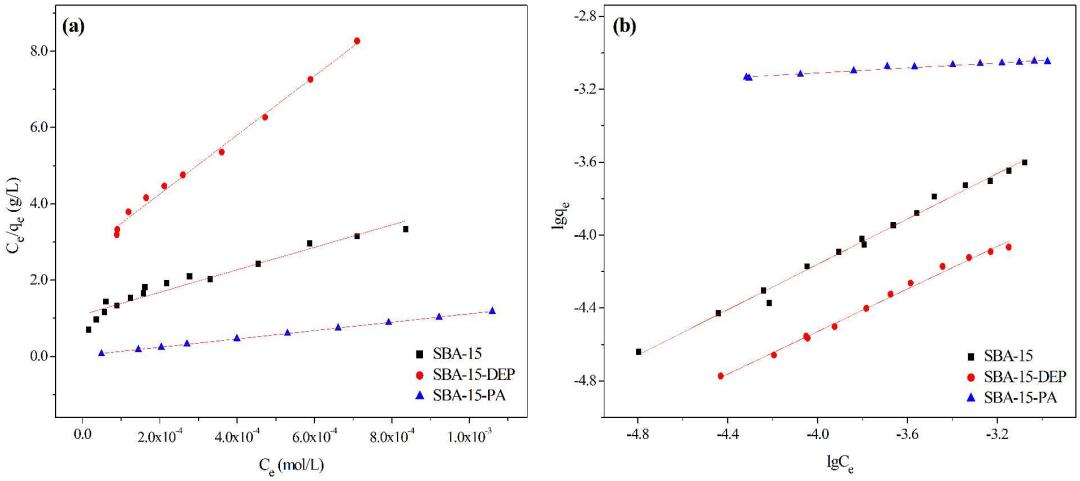

Fig.9.

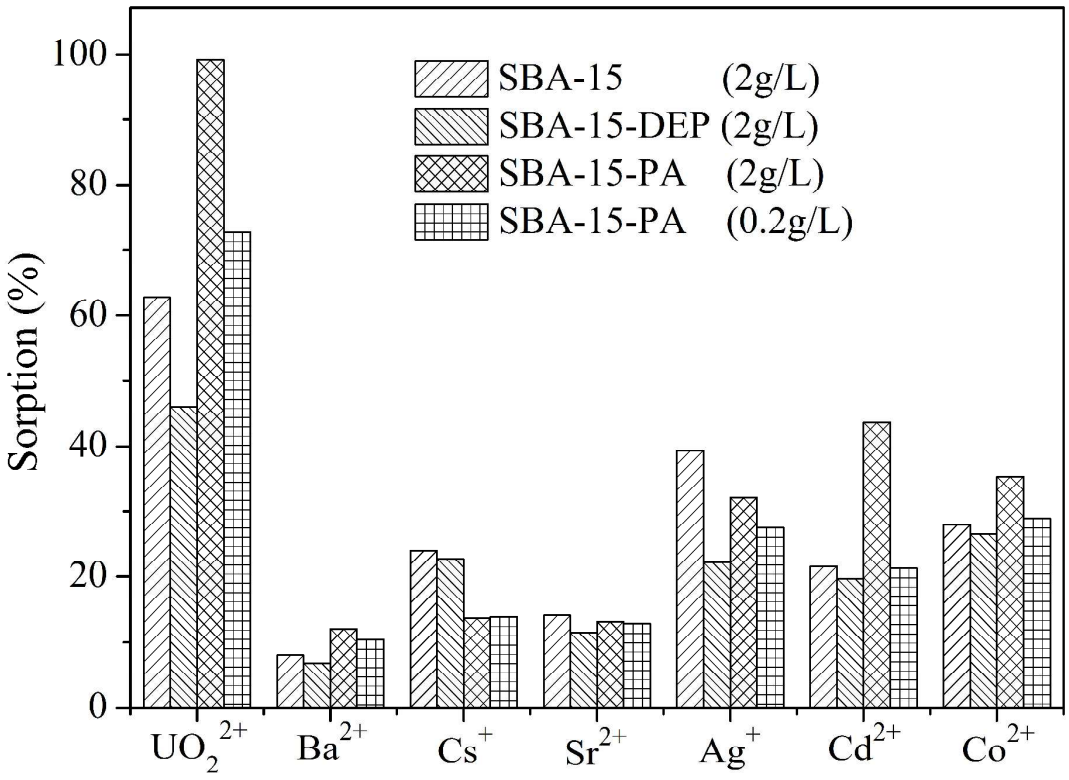

Fig.10.

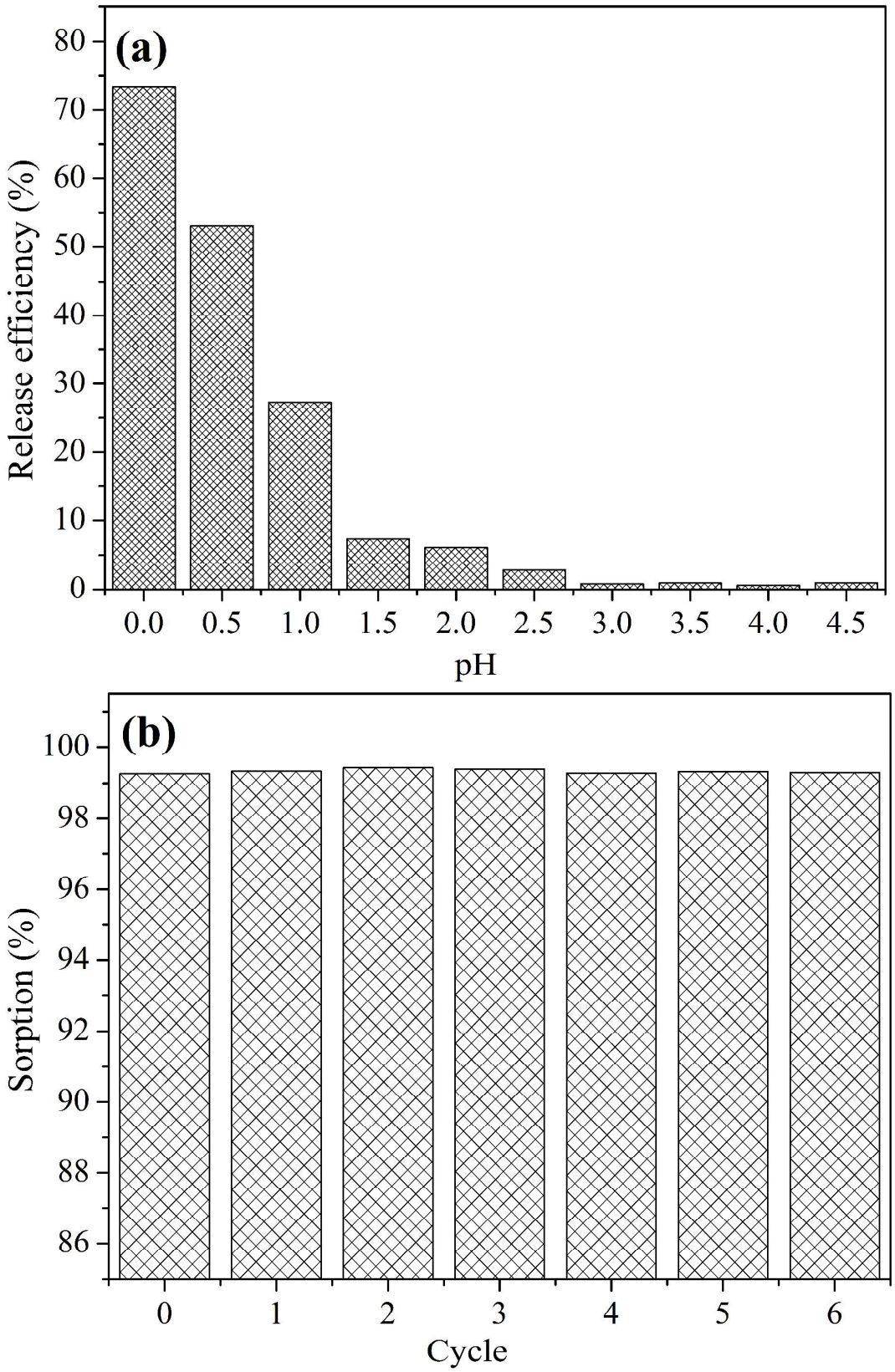

Fig.11.

Table 1. Physical properties of adsorbents.

	SBA-15	SBA-15-DEP	SBA-15-PA
BET (m^2/g)	815.7	502.9	494.6
Pore Volume (cm^3/g)	1.202	0.735	0.824
Pore Size (nm)	8.79	7.21	7.25

Table 2. Sorption parameters of U(VI) sorption to the adsorbents (298±1 K).

Samples	Langmuir constants			Freundlich constants		
	q_{max} (mol/g)	K_L (L/g)	R^2	K_F (mol^{1-n} L^n g^{-1})	n	R^2
SBA-15	3.39E-4	0.915	0.938	2.14E-2	0.623	0.991
SBA-15-DEP	1.29E-4	0.369	0.994	6.43E-3	0.584	0.993
SBA-15-PA	9.14E-4	44.37	1.000	1.46E-3	0.069	0.966